THE JOURNAL OF BIOLOGICAL CHEMISTRY VOL. 288, NO. 2, pp. 974–983, January 11, 2013
© 2013 by The American Society for Biochemistry and Molecular Biology, Inc. Published in the U.S.A.

Pak2 Kinase Restrains Mast Cell FcεRI Receptor Signaling through Modulation of Rho Protein Guanine Nucleotide Exchange Factor (GEF) Activity*

Received for publication, September 24, 2012, and in revised form, November 29, 2012 Published, JBC Papers in Press, November 30, 2012, DOI 10.1074/jbc.M112.422295

Rachelle Kosoff[‡§], **Hoi Yee Chow**[§], **Maria Radu**[§], **and Jonathan Chernoff**[§1]

From the [‡]*Cancer Biology Program, University of Pennsylvania, Philadelphia, Pennsylvania 19104 and the* [§]*Cancer Biology Program, Fox Chase Cancer Center, Philadelphia, Pennsylvania 19111*

Background: The protein kinase Pak1 stimulates mast cell degranulation, but the role of the more abundant isoform Pak2 in these cells is unknown.
Results: Pak2, unlike Pak1, inhibits mast cell degranulation via a GEF-H1-RhoA pathway.
Conclusion: Pak2 mediates signals between FcεRI and secretion through regulation of the GEF responsible for RhoA activation.
Significance: Pak2 has an opposing role to Pak1 in mast cell degranulation.

p21-activated kinase-1 (Pak1) is a serine/threonine kinase that plays a key role in mediating antigen-stimulated extracellular calcium influx and degranulation in mast cells. Another isoform in this kinase family, Pak2, is expressed at very high levels in mast cells, but its function is unknown. Here we show that Pak2 loss in murine bone marrow-derived mast cells, unlike loss of Pak1, induces increased antigen-mediated adhesion, degranulation, and cytokine secretion without changes to extracellular calcium influx. This phenotype is associated with an increase in RhoA-GTPase signaling activity to downstream effectors, including myosin light chain and p38^{MAPK}, and is reversed upon treatment with a Rho-specific inhibitor. Pak2, but not Pak1, negatively regulates RhoA via phosphorylation of the guanine nucleotide exchange factor GEF-H1 at an inhibitory site, leading to increased GEF-H1 microtubule binding and loss of RhoA stimulation. These data suggest that Pak2 plays a unique inhibitory role in mast cell degranulation by down-regulating RhoA via GEF-H1.

Mast cells are immune cells that reside in nearly all vascularized tissues, particularly in tissues in close contact with the outside environment. Mast cells are one of the first immune cells to interact with foreign allergens, and it is therefore critical that these cells respond immediately to antigen by secreting biologically active mediators to promote or down-regulate inflammation (1). Secretion or degranulation is regulated by antigenic challenge to the high affinity receptor for the Fc fragment of IgE (FcεRI). Upon antigenic challenge, a signaling cascade of phosphatases and kinases is activated that coordinates dynamic changes in the cytoskeleton to promote immediate release of preformed granules via vesicle translocation and fusion to the plasma membrane (1, 2). Despite significant knowledge of mast cell biology and allergen response, the downstream effectors that link the complete signaling cascade from FcεRI to degranulation remain poorly understood.

p21-activated kinases (Paks)[2] are serine/threonine protein kinases that are activated by small GTPases, Rac1 and Cdc42. Paks are known to regulate a variety of important cellular processes, including control of the cytoskeleton and proliferation (3, 4). Paks comprise a family of six enzymes that are categorized into two subgroups: Group A (Pak1–3) and Group B (Pak4–6). Group A Paks, in particular Pak1, have been much studied due to their role in processes that affect neoplastic growth (5–8). Given that degranulation requires complete cytoskeleton rearrangement, we examined the roles of Group A Pak members 1 and 2 in mast cell secretion.

Currently, there is limited research on the biological differences among the Pak Group A isoforms. Pak1 and Pak2 are broadly expressed and share many substrates in common, including c-Raf and Mek1 (3). However, despite extensive structural similarities, particularly in the protein kinase domain, hints are beginning to emerge that these two isoforms have distinct functions. Gene knock-outs in mice reveal that loss of *Pak1* is well tolerated, with notable defects only in subsets of immune cells, such as mast cells and macrophages, whereas loss of *Pak2* results in early embryonic lethality (9–12). In a breast carcinoma cell line (T47D), Pak1 and Pak2 regulate invasion by distinct signaling mechanisms: Pak1 via regulation of cofilin phosphorylation and Pak2 via regulation of RhoA GTPase activity (13). Similar results were reported by Bright *et al.* (8), who showed that in DU145 prostate carcinoma cells, Pak1 promotes the loss of cell-cell E-cadherin junctions, resulting in enhanced migration, whereas Pak2 does

* This work was supported, in whole or in part, by National Institutes of Health Grants R01 CA58836 and R01 CA098830 (to J. C.). This work was also supported by American Asthma Foundation Grant 08-0049 and an appropriation from the state of Pennsylvania.
[1] To whom correspondence should be addressed: Fox Chase Cancer Center, 333 Cottman Ave., Philadelphia, PA 19111. Tel.: 215-728-5319; Fax: 215-728-3616; E-mail: Jonathan.Chernoff@fccc.edu.

[2] The abbreviations used are: Pak, p21-activated kinase; BMMC, bone marrow-derived mast cells; CRIB, Cdc42 and Rac1 interactive binding domain; DNP-HSA, dinitrophenyl-human serum albumin; GEF, guanine nucleotide exchange factor; 4-HT, 4-hydroxytamoxifen; IL, interleukin; MLC, myosin light chain; PLCγ1, phospholipase Cγ1; ERM, Ezrin/Radixin/Moesin; MSCV, murine stem cell virus; MT, microtubule; PP2A, protein phosphatase 2A; RBD, Rhotekin-binding domain.

Downloaded from www.jbc.org at Istituto Superiore di Sanità, on April 1, 2013

not affect migration but instead regulates lamellipodia extensions.

We previously reported that *Pak1* loss in mouse bone marrow-derived mast cells (BMMCs) was associated with reduced MAPK phosphorylation (Erk1/2 and p38), resulting in impaired stem cell factor-mediated migration *in vitro* and *in vivo* (11). Pak1 was found to positively regulate IgE-mediated degranulation via regulation of extracellular calcium influx through modulation of F-actin rearrangement (10). Recent data indicate that Pak1 regulates mast cell cytoskeleton rearrangement and degranulation through a kinase-dependent interaction with the phosphatase PP2A, which regulates Ezrin/Radixin/Moesin (ERM) proteins that uncouple the plasma membrane from actin prior to degranulation (14). These studies suggested that Group A Paks play a positive role in mast cell secretion and would be beneficial targets in asthma-related diseases.

In this study, we generated a conditional *Pak2* knock-out animal to investigate the function of other Group A Paks in allergen-mediated secretion. Surprisingly, we found that Pak1 and Pak2 play distinct and, in some cases, opposing roles in mast cell secretion. In contrast to Pak1, we found that Pak2 is a negative regulator of secretion via phosphorylation and inactivation of GEF-H1, leading to RhoA GTPase inhibition. These studies establish vital but distinct roles for Pak1 and Pak2 in mast cell secretion.

EXPERIMENTAL PROCEDURES

Mice—Syngeneic *Pak2*$^{fl/fl}$ mice on mixed background (sv129/C57Bl/6) were used for experimentation. Animal care and experimental procedures were conducted on a protocol approved by the Fox Chase Cancer Center Institutional Animal Care and Use Committee.

Genotyping by PCR—Tail DNA was digested with DirectPCR lysis buffer (Viagen, Los Angeles, CA) for tails with proteinase K and used for polymerase chain reaction (PCR) designed to amplify DNA fragments from the WT and targeted *Pak1* and *Pak2* alleles. For *Pak1* genotyping, a common forward primer (5′-GCC CTT CAC AGG AGC TTA ATG A-3′) was used with a *Pak1*-specific reverse primer (5′-GAA AGG ACT GAA TCT AAT AGC A-3′) to amplify a 240-bp product from the WT allele and with a *neo*-specific reverse primer (5′-CAT TTG TCACGT CCT GCACGA-3′) to amplify a 360-bp product from the targeted allele.

For *Pak2*$^{fl/fl}$ genotyping, the forward primer was 5′-ATCTTCCCAGGCTCCTGACA-3′, and the reverse primer was 5′-TGAAGCTGCATCAATCTATTCTG-3′. WT mice demonstrate a 306-bp band, and floxed mice demonstrate a 391-bp band.

Cre Activation—A retroviral vector for Cre recombinase (MSCV-CRE-ERT2) under tamoxifen control was used to excise Pak2 (Addgene plasmid 22776) (15). Cre-ERT2 contains Cre-recombinase fused to the ligand-binding domain of a mutated estrogen receptor, which recognizes tamoxifen or its derivative 4-hydroxytamoxifen (4-HT). This construct permits tamoxifen-dependent Cre activity. Recombinant virus was produced by retroviral packaging into 293-FT cells and co-transfected using Lipofectamine 2000 with vectors pVPack gag-pol and pVPack eco (Stratagene, La Jolla, CA). Viral supernatant was collected 48 and 72 h after transfection. Transduction of bone marrow was performed within 1 week of extraction and performed by spin infection with 4 μg/ml Polybrene. At least two rounds of transduction were performed prior to the addition of puromycin for drug selection. 250 nM 4-HT was added to mature mast cells 4 days prior to experimentation. Western blot analysis confirmed deletion of Pak2 by 4 days.

Western Blotting—Whole-cell protein extracts after antigen stimulation were prepared by the addition of lysis buffer (50 mM Tris, pH 7.4, 150 mM NaCl, 2 mM EDTA, pH 8.0, 1% Triton X-100, 1 mM PMSF, 1 mM NaF, 1 mM Na_3VO_4, 10% glycerol, and Complete protease inhibitor (Sigma), clarified by centrifugation, and denatured with 1× SDS sample buffer. Samples were separated by SDS-polyacrylamide gel electrophoresis (PAGE) on a 4–20% gradient gel (Bio-Rad) and transferred to PVDF membrane. Blots were probed with anti-Pak1, anti-Pak2, anti-phospho-phospholipase Cγ1, anti-total phospholipase Cγ1, anti-phospho-myosin light chain 2, anti-total myosin light chain 2, anti-phospho-stathmin, anti-phospho-p38, anti-p38, anti-phospho-ERK1/2, anti-ERK1/2, and anti-GEF-H1 (all 1:1000, Cell Signaling, Danvers, MA). Anti-phospho-GEF-H1 (Ser-885) was a gift from Celine DerMardirossian. All blots were then visualized with HRP-conjugated goat anti-rabbit or anti-mouse IgG antibody (1:10000; Jackson ImmunoResearch Laboratories, West Grove, PA). Films were developed using enhanced chemiluminescence (ECL) (EMD Millipore). Phosphorylated proteins were quantified by subjecting autoradiographs to densitometry (NIH ImageJ software) and calculated relative to total protein. Bands were normalized to background, and the ratio of background-corrected raw intensities of protein of interest/total protein was calculated.

Cell Culture and Activation—BMMCs were cultured in RPMI (Invitrogen) supplemented with 15% fetal calf serum, 1% glutamine, 1.5% 1 M HEPES, 2% penicillin/streptomycin, 5 ng/ml recombinant murine interleukin-3 (IL-3), and 10 ng/ml stem cell factor (PeproTech, Rocky Hill, NJ). All cellular and biochemical assays used BMMCs that had been in culture between 4 and 10 weeks. All experiments were conducted using at least three independent lines from each genotype. BMMCs were sensitized in cytokine-free medium with 0.5 μg/ml anti-DNP IgE monoclonal antibody (clone SPE-7; Sigma-Aldrich) overnight and stimulated with 10 and 30 ng/ml dinitrophenyl conjugated to human serum albumin (DNP-HSA, 30–40 mol of DNP/mol HSA; Sigma-Aldrich) for degranulation assays and 100 ng/ml dinitrophenyl in phosphorylation and pulldown assays.

Detection of c-Kit/FcϵRI Receptors— c-Kit and FcϵRI expression were analyzed by fluorescence cytometry as described (16). Cells were blocked with unconjugated anti-FcγRII/III (BD Pharmingen) and stained with anti-DNP monoclonal antibody IgE clone SPE-7 (Sigma-Aldrich), anti-mouse CD 117 (c-Kit) phycoerythrin-conjugated antibody, and FITC-conjugated anti-mouse IgE (both BD Pharmingen) secondary antibody. Cells were washed and resuspended in 0.5% FBS, PBS buffer. Cells were analyzed on a FACSCalibur (BD Biosciences).

Degranulation—BMMC degranulation was determined by β-hexosaminidase release as described previously (17) with minor modification. IgE-primed (see "Cell Culture and Activa-

Downloaded from www.jbc.org at Istituto Superiore di Sanità, on April 1, 2013

tion") BMMCs were suspended at 5×10^6 cells/ml in HEPES-BSA buffer (10 mM HEPES buffer, 130 mM NaCl, 5 mM KCl, 1.4 mM $CaCl_2$, 1 mM $MgCl_2$, 5.6 mM glucose, 0.05% BSA, pH 7.4) and then stimulated with 10 or 30 ng/ml DNP-HSA (Sigma-Aldrich) for 45 min at 37 °C. For receptor-independent stimulation, unsensitized cells were incubated in HEPES-BSA buffer and stimulated with 1 μM ionomycin for 45 min. The cell pellets were solubilized in HEPES-BSA buffer, 0.5% Triton X-100. β-Hexosaminidase release was measured in both the supernatants and the cell pellets by incubating with 4-nitrophenyl *N*-acetyl-β-D-glucosaminide (Sigma-Aldrich) in sodium citrate (pH 4.5) for 1.5 h at 37 °C. Sodium carbonate/sodium bicarbonate buffer (0.1 M, pH 10) was used to stop the reaction, and absorbance was read at 405 nm. Degranulation was expressed as a percentage of β-hexosaminidase released = supernatant activity/total (supernatant plus pellet) activity $\times$ 100. Samples were assayed in triplicate.

ELISA—BMMC cytokine secretion was determined using ELISA for tumor necrosis factor-α (TNF-α) and IL-6 (eBioscience, San Diego, CA). Cells were sensitized overnight in cytokine-free medium with 0.5 μg/ml anti-DNP IgE. Cells were washed and stimulated with 30 ng/ml DNP-HSA for 6 h. Supernatants were collected, and cytokine release was measured. Cytokine release was normalized to phorbol 12-myristate 13-acetate and ionomycin treatment.

GTPase Pulldown Assays—Recombinant glutathione S transferase (GST)-conjugated PAK CRIB domain was expressed from pGEX-CRIB, and Rhotekin RBD-GST beads were acquired from Millipore. Cells were sensitized overnight in anti-DNP IgE (Sigma) without cytokines and stimulated with 100 ng/ml DNP-HSA for 10 min at 37 °C. Lysates were incubated with CRIB-GST or RBD-GST beads for 45 min rotating at 4 °C, washed, and run out on a 4–20% SDS-PAGE gel (Bio-Rad). Immunoblots of lysates incubated with beads and input were probed for anti-RhoA (Santa Cruz Biotechnology, Santa Cruz, CA), anti-Rac1 (BD Transduction Laboratories), or anti-Cdc42 (Cell Signaling). GTP-bound lane intensity was normalized to input lane intensity and calculated relative to unstimulated levels in wild-type cells using ImageJ (National Institutes of Health).

BMMC Adhesion Assay—BMMCs were starved of cytokines and sensitized overnight with anti-DNP-IgE (0.5 μg/ml). Cells were washed in HEPES-BSA buffer and placed in wells of a 96-well black microtiter plate (5×10^4 cells/well). Wells were precoated with 0.2% gelatin for 1 h and washed, and serum was added for 1 h at room temperature. This procedure resulted in a fibronectin coating of the wells. After 30 min of rest, cells were stimulated with DNP-HSA (1 or 10 ng/ml) for 45 min. 10 min prior to the end of the assay, the membrane-permeable viability dye calcein-AM (2 μg/ml) (eBioscience) was loaded onto the cells. A PerkinElmer Life Sciences Envision plate reader was used to measure fluorescence at 530 nm. First, wells were read to obtain a total fluorescence, after which they were washed, and bound cells were measured. Background fluorescence was subtracted, and the percentage of adherence was calculated by taking adherent cell fluorescence as a percentage of total well calcein-AM fluorescence. At least three individual mice were used per group, and assays were run in triplicate.

Calcium Mobilization—IgE-primed BMMCs were resuspended at 10^6 cells/ml in HEPES-BSA buffer containing Indo-1-AM (eBioscience) and probenecid at 37 °C for 1 h. Cells were washed and resuspended at 10^6 cells/ml in HEPES-BSA buffer. Samples were warmed to 37 °C, and base-line fluorescence was measured for 1 min. 30 ng/ml DNP-HSA was added to the cells, and the change in fluorescence (420 nm Ca^{2+}-bound, 510 nm Ca^{2+}-free) was monitored using the JSAN flow cytometer for 6 min. Positive controls were measured by stimulation with 1 μM thapsigargin. Data were graphed using FlowJo software (Tree-Star, Ashland, OR) and also used to analyze peak calcium flux normalized to base-line levels.

In Vitro Kinase Assay—HEK293 were transfected with pCDNA3-GEF-H1-GFP (gift from Celine DerMardirossian) using Lipofectamine 2000. Protein was purified using anti-GFP antibody (Santa Cruz Biotechnology) and conjugated to protein A/G-Sepharose beads (GE Healthcare). Protein was treated with λ-phosphatase (New England Biolabs) prior to use in the kinase assay. Immunoprecipitated GEF-H1 was incubated with recombinant Pak2 (ProQinase, Freiburg, Germany) and ATP in kinase buffer (40 mM HEPES, pH 7.5, 10 mM $MgCl_2$, 20 μM ATP) for 30 min at 30 °C. The reaction was fractionated on a 4–20% SDS-PAGE gel (Bio-Rad) and transferred to PVDF membrane. Membranes were probed for phospho-Ser-885 GEF-H1 (a gift from Celine DerMardirossian) and total GEF-H1 (Cell Signaling).

RESULTS

Genetic Disruption of Murine Pak2—Previously, we reported that Pak1 was a positive regulator of antigen-mediated degranulation in BMMCs via regulation of extracellular calcium flux (10). A closely related isoform, Pak2, is expressed at much higher levels than Pak1 (Fig. 1*A*) in mast cells; thus, we assessed the function of this kinase in antigen-mediated degranulation. Because the deletion of the *Pak2* gene is associated with embryonic lethality at approximately embryonic day 8 (12), we made a conditional knock-out of this gene. A targeting vector was designed to flank exon 2 of *Pak2* with *loxP* sites.

To confirm that the *Pak2* floxed alleles functioned as expected, bone marrow from $Pak2^{flox/flox}$ mice was infected with a tamoxifen-regulated Cre recombinase retrovirus (MSCV-Cre-ERT2). After maturation to mast cells, the cells were treated with 250 nM 4-HT for 4 days to excise *Pak2*. Protein extracts from these cells were immunoblotted and probed with anti-Pak2 antibodies (Fig. 1*B*). As expected, 4-HT-treated Cre-ERT2-infected cells showed near total loss of Pak2 protein. For comparison, immunoblots from $Pak1^{-/-}$ BMMCs are also shown. Deletion of either kinase did not affect protein levels of the other Pak isoform (data not shown).

Mast Cell Maturation from Pak1- and Pak2-deficient Mice—Bone marrow was cultured for 5 weeks with IL-3 and stem cell factor to derive mature mast cells. The development and maturation of these cells were measured using flow cytometry analysis of the cell surface receptors FcϵRI and c-Kit (CD117). Flow cytometry plots demonstrated over 90% FcϵRI$^+$ c-Kit$^+$ mature mast cells after 5 weeks of culture (Fig. 1*C*), irrespective of the presence or absence of Pak1 or Pak2 protein.

Downloaded from www.jbc.org at Istituto Superiore di Sanità, on April 1, 2013

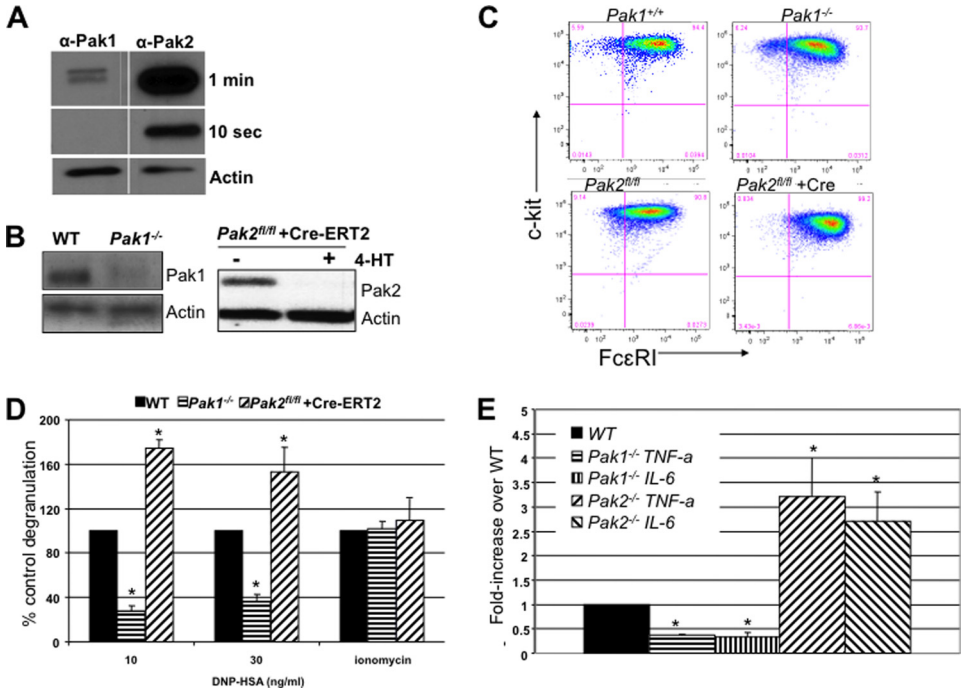

FIGURE 1. **Effect of Pak1 and Pak2 on mast cell maturation and antigen-mediated secretion.** *A*, WT MC-9 mouse mast cell line lysates were subjected to immunoblotting and probed with either anti-Pak1 or anti-Pak2 antibodies. Membranes were exposed together on the same film for the same amount of time for semiquantitative analysis. 10-s and 1-min exposures are shown, with loading control actin. *B*, BMMC lysates from *Pak1* knock-out mice and *Pak2*$^{fl/fl}$ infected with MSCV-Cre-ERT2 and treated with 250 nM 4-HT with actin loading control. *C*, loss of *Pak1* or *Pak2* does not affect expression of mast cell maturation markers. Mast cells were cultured for 4 weeks with cytokines, and expression of c-Kit and FcεRI was measured by FACS. Double-positive cells (*upper right quadrant*) are mature mast cells. Data shown are representative of six independent lines from each genotype. *D*, β-hexosaminidase release was measured in IgE-primed *Pak1* and *Pak2* knock-out BMMCs stimulated with 10 or 30 ng/ml DNP-HSA for 45 min. Average percentages of control of at least three independent experiments run in triplicate are shown here with standard deviations. FcεRI-independent degranulation is shown with ionomycin treatment. In all conditions, the extent of degranulation is represented as the percentage of total β-hexosaminidase activity in cells. *, p value < 0.05, Wilcoxon signed-rank test. *E*, ELISA was performed for TNF-α and IL-6 secreted by *Pak1* knock-out and *Pak2* knock-out BMMCs in response to 30 ng/ml DNP-HSA. Results are shown as average -fold change over WT cells for at least three independent experiments run in triplicate. *, p value < 0.05, Wilcoxon signed-rank test.

Thus, neither *Pak1* nor *Pak2* is essential for full maturation of bone marrow into mast cells *in vitro*.

Pak2 Is a Negative Regulator of Mast Cell Secretion—To examine the physiological responses of Pak2-deficient mast cells *in vitro*, we measured antigen-mediated degranulation and cytokine secretion. Previously, Pak1 was identified to regulate antigen-mediated degranulation *in vitro* (10). To determine whether Pak2 shares these properties, Pak2-deleted mast cells were sensitized with 0.5 μg/ml anti-DNP IgE overnight. The level of degranulation was measured by the amount of β-hexosaminidase release (an enzyme present in mast cell preformed granules). Surprisingly, *Pak2*-deleted mast cells showed a significant increase in degranulation (p value < 0.05, Wilcoxon signed-rank test) when compared with cells from the same mouse without Cre activation (infected with MSCV-Cre-ERT2; however, not given 4-HT) (Fig. 1*D*). Total enzyme content measured in the cell pellet was similar between *Pak2*$^{fl/fl}$ and *Pak2*$^{-/-}$ cells, indicating that *Pak2* deletion had no effect on the amount of β-hexosaminidase present, only on the release of granules. This finding is in stark contrast to *Pak1*-deleted mast cells, which had reduced degranulation (p value < 0.05, Wilcoxon signed-rank test), as reported previously (10) (Fig. 1*D*). To rule out nonspecific effects of Cre activation, Cre was activated in WT BMMCs and measured for degranulation. In these cells, no enhanced degranulation was observed (data not shown).

We also tested the response to ionomycin, a calcium ionophore used to activate store-operated calcium channels and initiate degranulation independent of antigen, and demonstrated no differences between genotypes. (Fig. 1*D*). Thus, our data show that Pak1 and Pak2 play opposing roles in IgE-mediated degranulation in mast cells; Pak1 positively regulates and Pak2 negatively regulates degranulation.

Activated mast cells also synthesize and secrete cytokines in response to antigen. We measured the release of IL-6 and TNF-α in FcεRI-activated mast cells by ELISA and found that *Pak1*$^{-/-}$ BMMCs were defective in secretion of IL-6 (p value $<$ 0.05, Wilcoxon signed-rank test) and TNF-α (p value < 0.05, Wilcoxon signed-rank test), consistent with the defect in degranulation (Fig. 1*E*). Alternatively, *Pak2*$^{-/-}$ BMMCs demonstrated significantly enhanced cytokine secretion for IL-6 (p value < 0.05, Wilcoxon signed-rank test) and TNF-α (p value $<$ 0.05, Wilcoxon signed-rank test) (Fig. 1*E*). These results show that, as with degranulation, Pak1 and Pak2 play opposing roles in IgE-mediated secretion of cytokines from mast cells.

FcεRI-dependent Calcium Mobilization Is Dependent on Pak1 but Not Pak2—The profound differences in regulation of degranulation between Pak1 and Pak2 in mast cells led us to examine differences along the signaling pathway leading to IgE-mediated degranulation. Antigen-induced phospholipase-Cγ1 (PLCγ1) activation leads to inositol 1,4,5-trisphosphate-dependent release of calcium from the endoplasmic reticulum, resulting in influx of extracellular calcium. Because neither loss of Pak1 nor loss of Pak2 was associated with alterations in phosphorylation of PLCγ1 at Tyr-783 (Fig. 2*A*), this lead us to exam-

Downloaded from www.jbc.org at Istituto Superiore di Sanità, on April 1, 2013

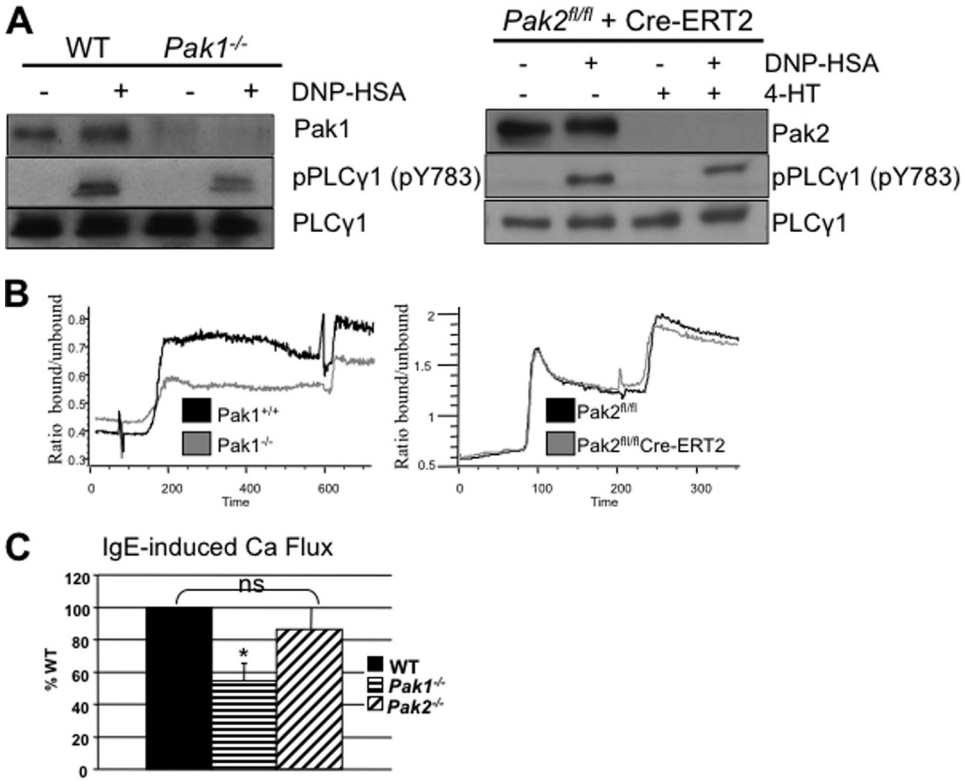

FIGURE 2. **Effect of Pak1 and Pak2 on calcium signaling and PLCγ1.** *A*, representative immunoblots for activated PLCγ1 in *Pak1* and *Pak2* knock-out BMMCs. IgE-primed WT and knock-out BMMCs were stimulated with DNP-HSA (100 ng/ml) for 3 min, and lysates were subjected to immunoblotting with anti-phospho-PLCγ1 phospho-Tyr-783 (*pPLCy1 pY783*, *middle panel*) or anti-total PLCγ1 (*bottom panel*). Experiments were done on three different mouse BMMCs. *Pak1* and *Pak2* status is shown for each blot (*top panel*). *B*, IgE-primed WT, *Pak1* knock-out and *Pak2* knock-out BMMCs were loaded with Ca^{2+}-sensitive dye (Indo-1-AM) and suspended in Ca^{2+}-containing medium. After base-line collection on JSAN flow cytometer, FcεRI was activated by the addition of 30 ng/ml DNP-HSA. The second stimulation peak is from thapsigargin treatment. Representative experiments of WT (*black*) *versus Pak1* knock-out (*gray*) (*left panel*) and *Pak2*$^{fl/fl}$ (*black*) *versus Pak2* knock-out (*gray*) (*right panel*) BMMCs are shown. *C*, mean (± S.D.) stimulation (peak of ratio minus base-line as the percentage of WT) of at least three independent experiments for *Pak1* knock-out and *Pak2* knock-out BMMCs. *Pak1* knock-out, *, p value < 0.05, Wilcoxon signed-rank test. Pak2 is not statistically different from WT. *ns*, not significant.

ine downstream events such as calcium influx. FcεRI signaling upon antigen stimulation results in calcium release from endoplasmic reticulum internal stores (first stage of Ca^{2+} mobilization) and subsequent prolonged influx of extracellular calcium (second stage of Ca^{2+} mobilization) through store-operated calcium release-activated calcium (CRAC) channels in the plasma membrane. Cells from all genotypes were sensitized with anti-DNP IgE and loaded with calcium-binding dye Indo-AM, and influx of extracellular calcium was measured by flow cytometry analysis by measuring Ca^{2+}-bound *versus* unbound Indo-AM after stimulation with antigen. When compared with their appropriate controls, *Pak1*-deleted BMMCs were significantly impaired for second stage calcium influx (Fig. 2, *B* and *C*; p value < 0.05, Wilcoxon signed-rank test), but had normal first stage release from the endoplasmic reticulum with antigen stimulation (10). *Pak2*-deleted BMMCs, however, were not defective in calcium influx from antigen stimulation (Fig. 2, *B* and *C*). These differences identify a key distinction in mast cell regulation between Pak1 and Pak2 in FcεRI-stimulated mast cells. These results collectively indicate that Pak1 and Pak2 play distinct roles in regulating calcium influx in FcεRI-stimulated BMMCs.

Pak1 and Pak2 Play Distinct Roles in IgE-mediated Adhesion—FcεRI receptor activation in mast cells not only leads to changes in secretion of inflammatory mediators, but also leads to increased adhesion (18). Mast cell activation of FcεRI receptor stimulates an increase in cell adhesion, and this adherence is required to facilitate localized synthesis of cytokines (19, 20). Given the role of Paks in cell migration, adhesion, and cytoskeleton regulation, we sought to discover a role for Paks in mast cell adhesion. Based on our data demonstrating altered secretion between the two genotypes, we hypothesized that Pak1 and Pak2 would differ in their effects on cell adhesion in response to antigen. Our findings demonstrated a significant reduction in antigen-mediated adhesion in *Pak1*$^{-/-}$ BMMCs (Fig. 3*A*, p value < 0.05, Student's t test) and a significant increase in adhesion in *Pak2*$^{-/-}$ BMMCs (Fig. 3*B*, p value < 0.05 Student's t test). We conclude from these data that differences observed between Pak1 and Pak2 in antigen-mediated secretion stem primarily from their opposing roles in adhesion.

Pak2 Regulates BMMC Secretion by Regulating RhoA GTPase Activity—RhoA GTPase activation is required for mast cell adhesion and secretion in response to IgE stimulation (21–23). Because Pak1 and Pak2 are thought to regulate RhoA by opposing mechanisms (13), we proceeded to investigate activation differences of RhoA in *Pak2*-deficient mast cells as a potential cause of enhanced secretion and adhesion. Using pulldown assays with the RhoA-binding domain, Rhotekin, we found that deletion of *Pak2* significantly increased the level of active GTP-

Downloaded from www.jbc.org at Istituto Superiore di Sanità, on April 1, 2013

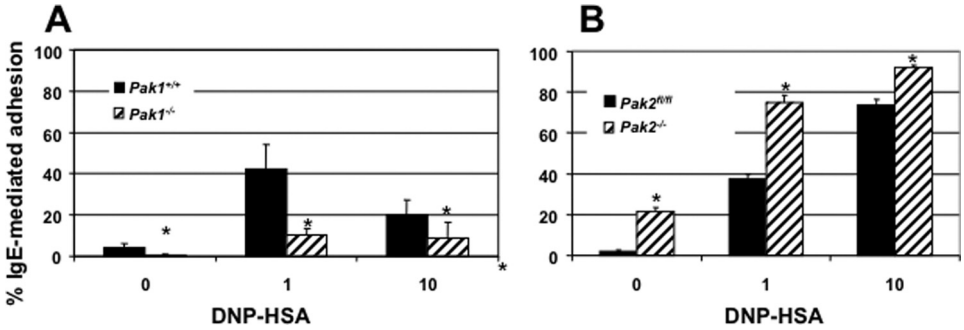

FIGURE 3. **Effect of Pak1 and Pak2 on adhesion.** *A*, the percentage of IgE-mediated adhesion in *Pak1* knock-out BMMCs on fibronectin-coated plates with 1 and 10 ng/ml DNP-HSA (*, p value < 0.05, Student's t test). *B*, the percentage of IgE-mediated adhesion in *Pak2* knock-out BMMCs (*, p value <0.05, Student's t test). Data are shown as the mean ± S.D. of at least three independent experiments run in triplicate. Data were calculated as the percentage of adhesion relative to total cells in each well using calcein-AM viability dye.

bound RhoA in antigen-stimulated cells (p value < 0.05 Student's t test) (Fig. 4*A*).

RhoA, through its effector Rho-associated, coiled coil-containing protein kinase (ROCK), phosphorylates and inactivates myosin phosphatase, leading to phosphorylation and activation of myosin light chain 2 (MLC2) (24). The active form of MLC2 was significantly elevated in *Pak2*$^{-/-}$ cells (p value < 0.05, Student's t test) (Fig. 4*B*). This finding is consistent with previous studies in breast cancer cells that showed elevated MLC2 phosphorylation when *Pak2* was silenced with siRNA (13).

If activated RhoA is responsible for the enhanced degranulation seen in *Pak2*$^{-/-}$ BMMCs, then pharmacologic inhibition of RhoA should block these effects. Inhibition of RhoA GTPase was achieved with *Clostridium botulinum* C3 exoenzyme (Cytoskeleton, Denver, CO), which selectively catalyzes the ADP-ribosylation and subsequent inactivation of RhoA, RhoB, and RhoC (25). Treatment of *Pak2*$^{-/-}$ BMMCs with C3 blocked the enhanced secretory phenotype in Pak2-null cells (p value < 0.05, Student's t test) (Fig. 4*C*). The phenotype observed in *Pak2*$^{-/-}$ BMMCs was RhoA-specific, and not due to elevated Rac1 or Cdc42, as deletion of *Pak2* did not affect Rac1-GTP or Cdc42-GTP levels as assessed by pulldown assay (Fig. 4*D*). Therefore, we conclude that Pak2 is a specific negative regulator of RhoA-GTPase activity in BMMCs.

Pak2 Negatively Regulates p38^{MAPK} *through RhoA Inhibition*—RhoA activates p38^{MAPK}, and this MAP kinase is known to regulate degranulation in mast cells (26). Pak1 was previously found to regulate p38^{MAPK} in stem cell factor-c-Kit receptor signaling (11). Based on this evidence, we asked whether Pak2 loss affected p38 activation by IgE engagement. We observed that loss of Pak2 resulted in a pronounced activation of p38^{MAPK} in response to antigen, with ~1.5-fold induction over WT cells at 2 and 5 min after stimulation (Fig. 5*A*, p value $<$ 0.05, Student's t test). The addition of the p38 inhibitor, SB203580 (Millipore), reduced the enhanced degranulation phenotype observed in *Pak2*$^{-/-}$ BMMCs (Fig. 5*B*, p value $<$ 0.05, Student's t test). These results, along with the observed effects on RhoA shown in Fig. 4*A*, suggest that Pak2 affects degranulation via a RhoA/p38-specific pathway as Pak2 loss had no effect on Erk1/2 activity (Fig. 5*C*). These data are in sharp contrast to those reported for Pak1, which, in BMMCs, serves as an activator of p38 and Erk1/2 (11).

Pak2 Regulates RhoA Activation via Phosphorylation and Inactivation of GEF-H1—How does Pak2 suppress RhoA activation? To answer this question, we looked toward the phosphorylation status of a known regulator of RhoA GTPase activity, GEF-H1. GEFs (guanine nucleotide exchange factors) convert RhoA-GDP to RhoA-GTP. The RhoA-specific GEF-H1 can only activate RhoA in the nonphosphorylated state. When phosphorylated at Ser-885, GEF-H1 localizes to microtubules and is inactivated, leading to inactive RhoA (27, 28). Pak1 was previously found to regulate GEF-H1 through phosphorylation at Ser-885, which induces 14-3-3 binding to GEF-H1 and relocation to the microtubules (29). As shown in Fig. 6*A*, when *Pak2* is deleted in BMMCs, phosphorylation of GEF-H1 is nearly abolished (p value < 0.05, Student's t test). *Pak1* deletion, in contrast, did not affect GEF-H1 phosphorylation (Fig. 6*C*). As impaired phosphorylation at Ser-885 is associated with constitutively active GEF-H1 and subsequent enhanced RhoA activity (30), it is likely that the observed impairment of GEF-H1 phosphorylation in *Pak2*-deleted cells is driving enhanced secretion. Interestingly, another Pak substrate associated with microtubules, stathmin/Op18, was also underphosphorylated at Ser-16 in *Pak2*$^{-/-}$ cells (Fig. 6*B*, p value < 0.05 Student's t test). Underphosphorylated stathmin/Op18 in *Pak2* null cells resulted in activated stathmin/Op18 and microtubule depolymerization. *Pak1*-null cells fail to show a defect in either GEF-H1 or stathmin phosphorylation, indicating in mast cells that these are specific downstream targets of Pak2. Finally, a kinase assay to assess the ability of Pak2 to directly phosphorylate GEF-H1 at Ser-885 demonstrates that GEF-H1 can be phosphorylated by Pak2 *in vitro* (Fig. 6*E*). Together these data demonstrate that Pak2 regulates RhoA-GTPase via regulation of microtubule-associated proteins, and this regulation mediates mast cell FcϵRI responses independent of the effects of Pak1.

DISCUSSION

In this study, we describe the distinct functional roles of Pak1 and Pak2 in allergen-induced bone marrow-derived mast cell degranulation. Previously, we reported that Pak1 in mast cells modulates allergen- and stem cell factor-induced F-actin rearrangement and degranulation (10, 11). Pak1 was recently found to regulate mast cell secretion by promoting assembly of a PP2A phosphatase complex (14). This phosphatase complex

Downloaded from www.jbc.org at Istituto Superiore di Sanità, on April 1, 2013

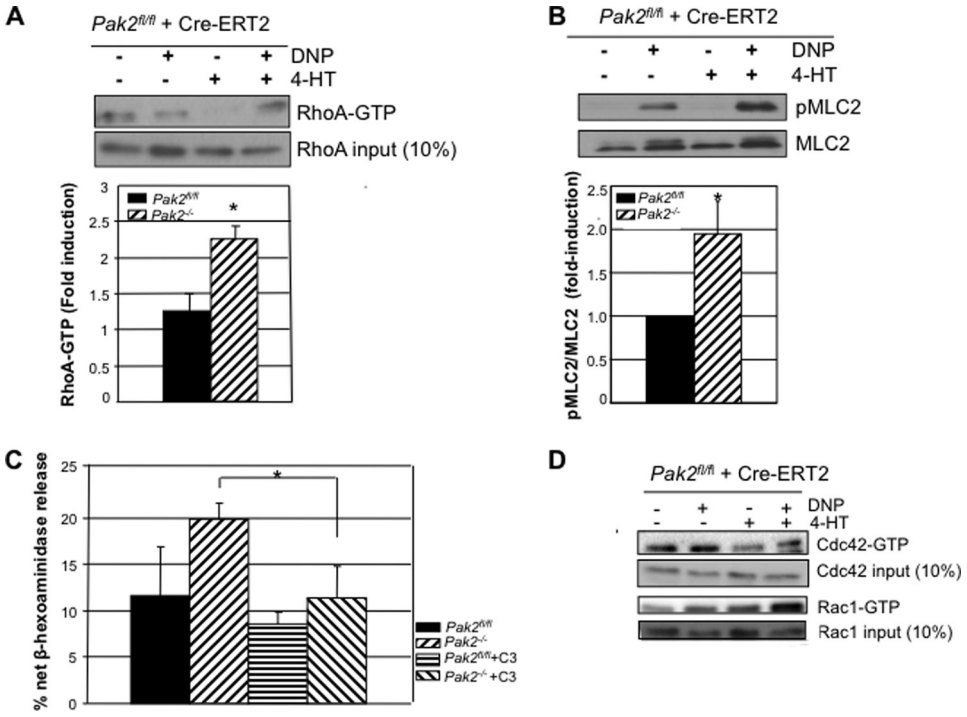

FIGURE 4. **Effect of Pak2 on Rho GTPase activity.** *A*, IgE-primed *Pak2*$^{fl/fl}$ and *Pak2*$^{-/-}$ BMMCs were stimulated with 100 ng/ml DNP-HSA for 10 min, and lysates were cleared and incubated with Rhotekin RBD-GST beads (Millipore). RhoA-GTP was detected by anti-RhoA antibody, and 10% of input demonstrates equal loading. One representative Western blot of three experiments is shown, and densitometry of the -fold induction relative to unstimulated cells (all normalized to input) of three independent experiments is shown (*, p value < 0.05, Student's t test). *B*, activation status of MLC2, a downstream RhoA effector, at p-Thr-18/Ser-19 in lysates from 10 min of DNP-HSA stimulation. The blot is representative of three separate experiments, and densitometry shows average -fold ($\pm$ S.D.) change over stimulated wild-type cells normalized to total MLC2 for three independent experiments (*, p value < 0.05, Student's t test). *pMLC2*, phospho-MLC2. *C*, C3 exoenzyme, a RhoA inhibitor, was treated on *Pak2*$^{fl/fl}$ and *Pak2*$^{-/-}$ BMMCs for 6 h without serum. A degranulation assay was performed with 30 ng/ml DNP-HSA. The graph is an average of three independent experiments run in triplicate with S.D. (*, p value < 0.05, *Pak2*$^{-/-}$ *versus Pak2*$^{-/-}$ +C3, Student's t test). *D*, Rac1 and Cdc42 activity (GTP-bound isoforms) of *Pak2*$^{fl/fl}$ and *Pak2*$^{-/-}$ BMMCs after DNP-HSA stimulation for 10 min (representative blot of three independent BMMCs). Total Rac1 and Cdc42 proteins for each sample before performing pulldown are detected with monoclonal anti-Rac1 and polyclonal anti-Cdc42.

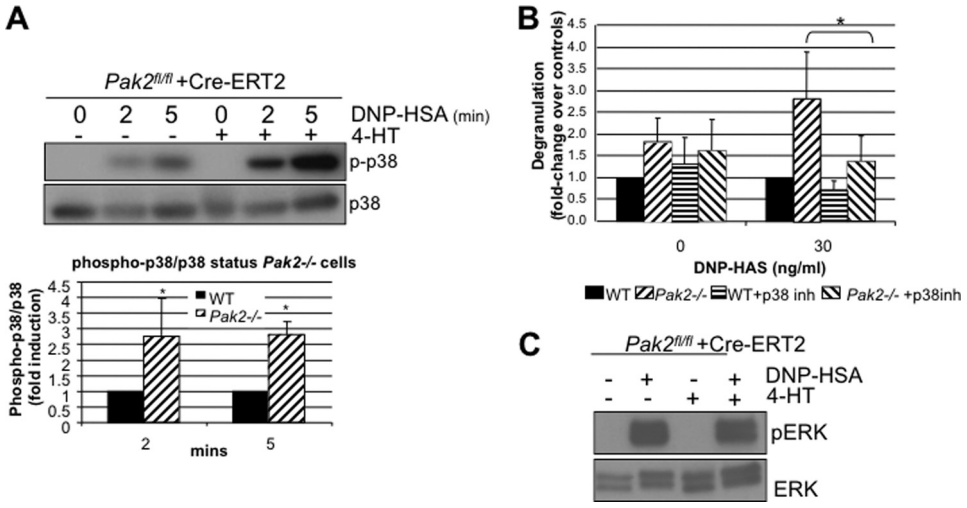

FIGURE 5. **Effect of Pak2 on MAPK activity.** *A*, IgE-primed *Pak2*$^{fl/fl}$ and *Pak2*$^{-/-}$ BMMCs were stimulated with 100 ng/ml DNP-HSA for 0, 2, 5, and 10 min, and lysates were cleared and immunoblotted for anti-phospho-p38 (Thr-180/182), and anti-total p38. A representative blot is shown above, and below are shown the average of three independent experiments and standard deviations for relative -fold induction over wild-type cells for phospho-p38 (*p-p38*)/total p38. (*, p value <0.05, Student's t test) *B*, degranulation of IgE-primed *Pak2*$^{fl/fl}$ and *Pak2*$^{-/-}$ BMMCs stimulated with 30 ng/ml DNP-HSA antigen and incubated with p38 inhibitor SB203580 (10 μM) 30 min prior to assay. Average -fold change of three independent experiments and standard deviations (*, p value < 0.05, Student's t test) are shown. *C*, ERK1/2 was probed on immunoblots from *Pak2*$^{fl/fl}$ and *Pak2*$^{-/-}$ stimulated for 10 min with 100 ng/ml DNP-HSA antigen. A representative blot is shown, run for three independent experiments. *pERK*, phospho-ERK.

dephosphorylates ERM, resulting in uncoupling of the actin cytoskeleton from the plasma membrane and subsequent degranulation. Here we show that disruption of the *Pak2* gene in BMMCs increases the allergen-induced degranulation response, opposing Pak1 function. These results demonstrate that Pak2 is a negative regulator of secretion. Pak1 and Pak2 share high structural homology within their catalytic domains. Pak2, however, is the predominant isoform in BMMCs, sug-

Downloaded from www.jbc.org at Istituto Superiore di Sanità, on April 1, 2013

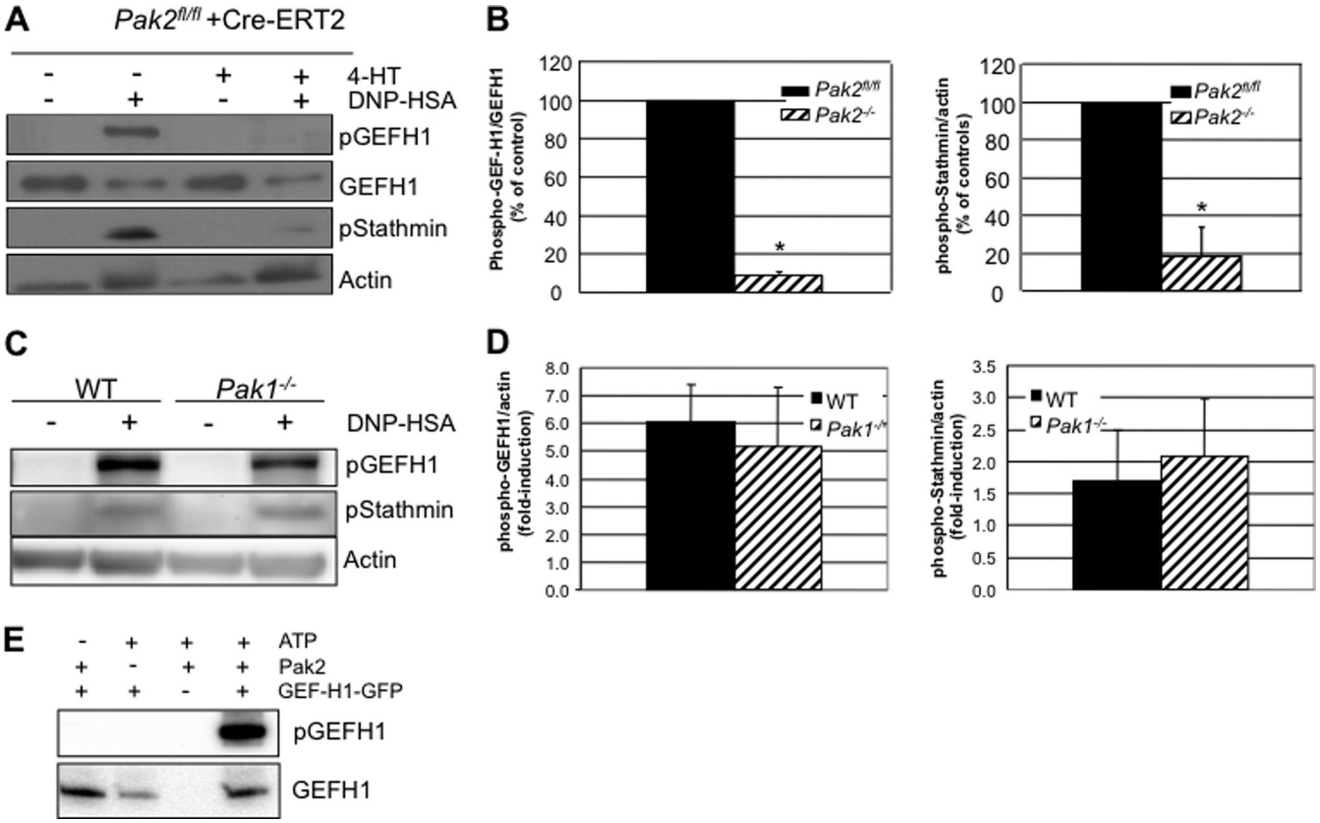

FIGURE 6. **Pak2 and MT protein phosphorylation.** *A*, IgE-primed *Pak2*$^{fl/fl}$ and *Pak2*$^{-/-}$ BMMCs were stimulated with 100 ng/ml DNP-HSA for 10 min, and lysates were cleared and immunoblotted for phospho-GEF-H1 (*pGEFH1*) (Ser-885), total GEF-H1, phospho-stathmin (*pStathmin*) (Ser-16), and actin (loading control). Representative blots are shown. *B*, *left panel*, the graph depicts the average of three independent experiments and standard deviations for the percentage of change in phospho-GEF-H1 (Ser-885), normalized to total GEF-H1 (*, p value < 0.05, Student's t test). *Right panel*, the graph depicts the average of three independent experiments and standard deviations for the percentage of change in phospho-stathmin (Ser-16) normalized to actin, relative to WT cells (*, p value < 0.05, Student's t test). *C*, representative blot of IgE-primed *Pak1*$^{-/-}$ BMMCs stimulated with 100 ng/ml DNP-HSA for 10 min. Lysates were cleared and immunoblotted for phospho-GEFH1 (Ser-885), phospho-stathmin (Ser-16), and actin (loading control). *D*, the graph depicts -fold induction of phospho-GEFH1 and phospho-stathmin normalized to actin, average of three independent experiments, and standard deviations. *E*, *in vitro* kinase assay with recombinant Pak2 and GEF-H1-GFP; lysates run on parallel membranes were probed with anti-phospho-GEF-H1 (Ser-885) and anti-GEF-H1.

gesting that small molecule Pak inhibitors would most likely demonstrate a Pak2 phenotype in mast cells, possibly resulting in severe anaphylaxis (31–33). These findings also point to our limited understanding of the differences between Pak1 and Pak2 in terms of regulation and substrate specificity.

Unlike *Pak1* loss, *Pak2* loss resulted in elevated RhoA-GTPase activity, leading to enhanced MLC2 phosphorylation, adhesion, secretion, and p38 activity. Previously, *Pak1* and *Pak2* inhibition with siRNA demonstrated that they play distinct roles in focal adhesions, mediated in part through their different regulation of MLC phosphorylation (13). *Pak1* loss resulted in decreased MLC phosphorylation and failure to form focal adhesions, whereas *Pak2* loss resulted in elevated MLC activity, leading to significantly larger focal adhesions. As shown here, *Pak2*-null, but not *Pak1*-null, BMMCs had elevated MLC phosphorylation, most likely secondary to activation of the RhoA signaling pathway. Consistent with this view, the addition of a RhoA inhibitor, C3 exoenzyme, was sufficient to rescue the *Pak2*-deficient mast cells to WT levels of degranulation. Downstream of RhoA, p38^{MAPK} is required for degranulation (26), and we found that drug inhibition of p38 in *Pak2*-deficient mast cells rescued the enhanced degranulation phenotype to WT levels (Fig. 5*B*). These data demonstrate that Pak2 is a negative regulator of the RhoA/p38 signaling axis in mast cells.

Regulation of RhoA activity by Pak2 could be mediated by GTPase-activating proteins (GAPs), GEFs, and/or guanine nucleotide dissociation inhibitors (GDIs). Because GEF-H1 was previously shown to be inhibited by phosphorylation by Pak1 and Pak4, we evaluated the role of Pak2 on GEF-H1 phosphorylation (29, 32, 34). Phosphorylation of GEF-H1 was greatly inhibited in *Pak2*-deficient BMMCs. Phosphorylation of GEF-H1 at Ser-885 is known to promote its localization to microtubules by binding 14-3-3, leading to inhibition of its exchange activity (27–29). These results suggest that in the absence of Pak2, GEF-H1 remains underphosphorylated and in the active state, thereby activating RhoA. Activated RhoA promotes enhanced degranulation in *Pak2*-deficient cells, as shown by the finding that enhanced degranulation was abolished by the addition of the RhoA inhibitor, C3 exoenzyme (Fig. 4*C*). An *in vitro* kinase assay demonstrated that Pak2 directly phosphorylates GEF-H1 at Ser-885 (Fig. 6*E*). Together these data suggest that Pak2 regulates GEF-H1 through phosphorylation to negatively regulate mast cell degranulation.

A previously identified target of Pak1, stathmin/Op18, functions to destabilize microtubules when in the unphosphorylated state by sequestering α- and β-tubulin dimers (35). Stathmin/Op18 also functions as a relay in various signal transduction pathways for extracellular signals and to regulate the MT

Downloaded from www.jbc.org at Istituto Superiore di Sanità, on April 1, 2013

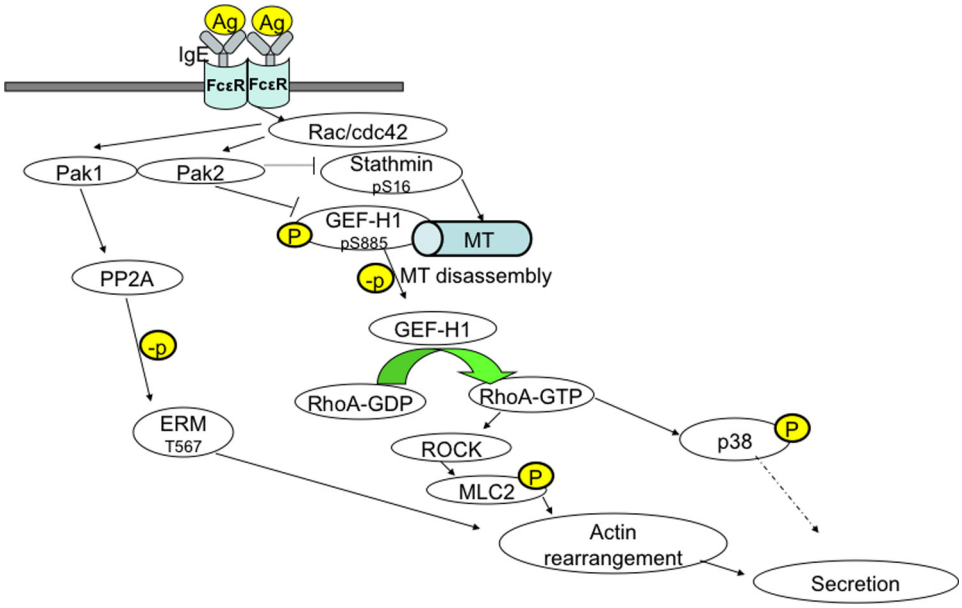

FIGURE 7. **Model of Pak2 signaling in mast cells.** A model demonstrating how Pak1 and Pak2 regulate IgE-mediated secretion in bone marrow-derived mast cells is shown. In this scenario, Pak1 and Pak2 play opposing roles. Pak1, which is present at lower levels than Pak2 in mast cells, acts through association with PP2A to promote ERM phosphorylation and augment secretion. Pak2 acts primarily through phosphorylation of GEF-H1 and stathmin/Op18 to limit RhoA activity, leading to diminished downstream activation of p38 and MLC2. Limiting the activity of these effectors results in diminished secretion. Differential spatial or temporal regulation of Pak1 *versus* Pak2 might determine the output (*i.e.* secretion or no secretion) under particular conditions. *Ag*, antigen; *p*, phosphorylation; *MT*, microtubule.

network (36). Stathmin/Op18 requires proximity to assembling MTs to become locally phosphorylated (37). Many kinases and phosphatases, including ERK, are associated with microtubules and therefore function only with intact MTs. Some kinases are activated in response to a change in the cellular MT network. In this context, it is interesting to note that Pak1 is a known negative regulator of stathmin via phosphorylation at Ser-16, a site critical for the microtubule-depolymerizing activity of stathmin/Op18 (38). We found that this site was underphosphorylated in *Pak2*-deficient cells, but not in *Pak1*-deficient BMMCs, suggesting that stathmin is constitutively active in *Pak2*-deficient mast cells, destabilizing MTs and driving degranulation.

These results suggest two hypotheses to explain Pak2 function in mast cells. First, Pak2 could regulate RhoA activity in mast cells directly by phosphorylation of GEF-H1 at Ser-885, resulting in inhibition of this GEF with subsequent reduction in RhoA activity (Fig. 6*E*). In addition, Pak2 might affect GEF-H1 indirectly through phosphorylation of stathmin, resulting in inhibition of stathmin, stabilization of MTs, and retention of inactive GEF-H1 at these stabilized MTs (Fig. 7). In *Pak2*$^{-/-}$ cells, underphosphorylated stathmin drives MT disassembly, generating active GEF-H1, leading to elevated RhoA activity and driving secretion. These two hypotheses are not mutually exclusive.

What accounts for the opposing signaling effects of Pak1 and Pak2 in mast cells? These two kinases have very similar N-terminal p21-binding domains and C-terminal protein kinase domains and have many binding partners and substrates in common. However, the primary intracellular localization of these two enzymes may differ (39, 40). For example, Pak1, unlike Pak2, is localized to cytosolic vesicular structures in unstimulated cells and translocates to the nucleus following growth factor stimulation (41, 42). This unique feature may impart unique functions to Pak1. With respect to GEF-H1 phosphorylation, Pak1 (and Pak4) has been reported to catalyze Ser-885 phosphorylation, but perhaps due to its low abundance when compared with Pak2 in mast cells, it plays little role in regulating GEF-H1 in this cell type (Fig. 6, *C* and *D*). In contrast, despite its relative low abundance in mast cells, Pak1, but not Pak2, is required for normal Erk activation (Fig. 5*C*) (11). Experiments that employ chimeric versions of Pak1/2 hybrids may in the future prove useful in mapping structural features within these kinases that impart signaling specificity.

Acknowledgments—We thank Celine DerMardirossian for anti-phospho-GEF-H1 antibodies and plasmid constructs and the Flow Cytometry Facility at Fox Chase for assistance with analysis of calcium signaling. The Fox Chase Cancer Center was supported by National Institutes of Health Grant P30 CA006927.

REFERENCES

1. Galli, S. J., and Tsai, M. (2012) IgE and mast cells in allergic disease. *Nat. Med.* **18,** 693–704
2. Galli, S. J., Kalesnikoff, J., Grimbaldeston, M. A., Piliponsky, A. M., Williams, C. M. M., and Tsai, M. (2005) Mast cells as "tunable" effector and immunoregulatory cells: Recent advances. *Annu. Rev. Immunol.* **23,** 749–786
3. Bokoch, G. M. (2003) Biology of the p21-activated kinases. *Annu. Rev. Biochem.* **72,** 743–781
4. Molli, P. R., Li, D. Q., Murray, B. W., Rayala, S. K., and Kumar, R. (2009) PAK signaling in oncogenesis. *Oncogene* **28,** 2545–2555
5. Dummler, B., Ohshiro, K., Kumar, R., and Field, J. (2009) Pak protein kinases and their role in cancer. *Cancer Metastasis Rev.* **28,** 51–63
6. Eswaran, J., Soundararajan, M., Kumar, R., and Knapp, S. (2008) UnPAKing the class differences among p21-activated kinases. *Trends Biochem. Sci.* **33,** 394–403
7. Arias-Romero, L. E., and Chernoff, J. (2008) A tale of two Paks. *Biol. Cell* **100,** 97–108

Downloaded from www.jbc.org at Istituto Superiore di Sanità, on April 1, 2013

8. Bright, M. D., Garner, A. P., and Ridley, A. J. (2009) PAK1 and PAK2 have different roles in HGF-induced morphological responses. *Cell Signal.* **21,** 1738–1747
9. Hofmann, C., Shepelev, M., and Chernoff, J. (2004) The genetics of Pak. *J. Cell Sci.* **117,** 4343–4354
10. Allen, J. D., Jaffer, Z. M., Park, S.-J., Burgin, S., Hofmann, C., Sells, M. A., Chen, S., Derr-Yellin, E., Michels, E. G., McDaniel, A., Bessler, W. K., Ingram, D. A., Atkinson, S. J., Travers, J. B., Chernoff, J., and Clapp, D. W. (2009) p21-activated kinase regulates mast cell degranulation via effects on calcium mobilization and cytoskeletal dynamics. *Blood* **113,** 2695–2705
11. McDaniel, A. S., Allen, J. D., Park, S.-J., Jaffer, Z. M., Michels, E. G., Burgin, S. J., Chen, S., Bessler, W. K., Hofmann, C., Ingram, D. A., Chernoff, J., and Clapp, D. W. (2008) Pak1 regulates multiple c-Kit mediated Ras-MAPK gain-in-function phenotypes in $Nf1^{+/-}$ mast cells. *Blood* **112,** 4646–4654
12. Smith, S. D., Jaffer, Z. M., Chernoff, J., and Ridley, A. J. (2008) PAK1-mediated activation of ERK1/2 regulates lamellipodial dynamics. *J. Cell Sci.* **121,** 3729–3736
13. Coniglio, S. J., Zavarella, S., and Symons, M. H. (2008) Pak1 and Pak2 mediate tumor cell invasion through distinct signaling mechanisms. *Mol. Cell Biol.* **28,** 4162–4172
14. Staser, K., Shew, M. A., Michels, E. G., Mwanthi, M. M., Yang, F.-C., Clapp, D. W., and Park, S.-J. (October 11, 2012) A Pak1-PP2A-ERM signaling axis mediates F-actin rearrangement and degranulation in mast cells. *Exp. Hematol.* 10.1016/j.exphem.2012.10.001
15. Kumar, M. S., Pester, R. E., Chen, C. Y., Lane, K., Chin, C., Lu, J., Kirsch, D. G., Golub, T. R., and Jacks, T. (2009) Dicer1 functions as a haploinsufficient tumor suppressor. *Genes Dev.* **23,** 2700–2704
16. Yang, F.-C., Kapur, R., King, A. J., Tao, W., Kim, C., Borneo, J., Breese, R., Marshall, M., Dinauer, M. C., and Williams, D. A. (2000) Rac2 stimulates Akt activation affecting BAD/Bcl-XL expression while mediating survival and actin function in primary mast cells. *Immunity* **12,** 557–568
17. Nishizumi, H., and Yamamoto, T. (1997) Impaired tyrosine phosphorylation and Ca^{2+} mobilization, but not degranulation, in lyn-deficient bone marrow-derived mast cells. *J. Immunol.* **158,** 2350–2355
18. Thompson, H. L., Burbelo, P. D., and Metcalfe, D. D. (1990) Regulation of adhesion of mouse bone marrow-derived mast cells to laminin. *J. Immunol.* **145,** 3425–3431
19. Dastych, J., and Metcalfe, D. D. (1994) Stem cell factor induces mast cell adhesion to fibronectin. *J. Immunol.* **152,** 213–219
20. Thompson, H. L., Thomas, L., and Metcalfe, D. D. (1993) Murine mast cells attach to and migrate on laminin-, fibronectin-, and Matrigel-coated surfaces in response to FcεRI-mediated signals. *Clin. Exp. Allergy* **23,** 270–275
21. Sullivan, R., Price, L. S., and Koffer, A. (1999) Rho controls cortical F-actin disassembly in addition to, but independently of, secretion in mast cells. *J. Biol. Chem.* **274,** 38140–38146
22. Norman, J. C., Price, L. S., Ridley, A. J., and Koffer, A. (1996) The small GTP-binding proteins, Rac and Rho, regulate cytoskeletal organization and exocytosis in mast cells by parallel pathways. *Mol. Biol. Cell* **7,** 1429–1442
23. Price, L. S., Norman, J. C., Ridley, A. J., and Koffer, A. (1995) The small GTPases Rac and Rho as regulators of secretion in mast cells. *Curr. Biol.* **5,** 68–73
24. Totsukawa, G., Yamakita, Y., Yamashiro, S., Hartshorne, D. J., Sasaki, Y., and Matsumura, F. (2000) Distinct roles of Rock (Rho-kinase) and Mlck in spatial regulation of Mlc phosphorylation for assembly of stress fibers and focal adhesions in 3t3 fibroblasts. *J. Cell Biol.* **150,** 797–806
25. Sekine, A., Fujiwara, M., and Narumiya, S. (1989) Asparagine residue in the *rho* gene product is the modification site for botulinum ADP-ribosyltransferase. *J. Biol. Chem.* **264,** 8602–8605
26. Gibbs, B. F., Plath, K. E. S., Wolff, H. H., and Grabbe, J. (2002) Regulation of mediator secretion in human basophils by p38 mitogen-activated protein kinase: phosphorylation is sensitive to the effects of phosphatidylinositol 3-kinase inhibitors and calcium mobilization. *J. Leukocyte Biol.* **72,** 391–400
27. Krendel, M., Zenke, F. T., and Bokoch, G. M. (2002) Nucleotide exchange factor GEF-H1 mediates cross-talk between microtubules and the actin cytoskeleton. *Nat. Cell Biol.* **4,** 294–301
28. Meiri, D., Marshall, C. B., Greeve, M. A., Kim, B., Balan, M., Suarez, F., Bakal, C., Wu, C., Larose, J., Fine, N., Ikura, M., and Rottapel, R. (2012) Mechanistic insight into the microtubule and actin cytoskeleton coupling through dynein-dependent RhoGEF inhibition. *Mol. Cell* **45,** 642–655
29. Zenke, F. T., Krendel, M., DerMardirossian, C., King, C. C., Bohl, B. P., and Bokoch, G. M. (2004) p21-activated kinase 1 phosphorylates and regulates 14-3-3 binding to GEF-H1, a microtubule-localized Rho exchange factor. *J. Biol. Chem.* **279,** 18392–18400
30. Yamahashi, Y., Saito, Y., Murata-Kamiya, N., and Hatakeyama, M. (2011) Polarity-regulating kinase partitioning-defective 1b (PAR1b) phosphorylates guanine nucleotide exchange factor H1 (GEF-H1) to regulate RhoA-dependent actin cytoskeletal reorganization. *J. Biol. Chem.* **286,** 44576–44584
31. Guo, C., McAlpine, I., Zhang, J., Knighton, D. D., Kephart, S., Johnson, M. C., Li, H., Bouzida, D., Yang, A., Dong, L., Marakovits, J., Tikhe, J., Richardson, P., Guo, L. C., Kania, R., Edwards, M. P., Kraynov, E., Christensen, J., Piraino, J., Lee, J., Dagostino, E., Del-Carmen, C., Deng, Y.-L., Smeal, T., and Murray, B. W. (2012) Discovery of pyrroloaminopyrazoles as novel PAK inhibitors. *J Med. Chem.* **55,** 4728–4739
32. Murray, B. W., Guo, C., Piraino, J., Westwick, J. K., Zhang, C., Lamerdin, J., Dagostino, E., Knighton, D., Loi, C.-M., Zager, M., Kraynov, E., Popoff, I., Christensen, J. G., Martinez, R., Kephart, S. E., Marakovits, J., Karlicek, S., Bergqvist, S., and Smeal, T. (2010) Small-molecule p21-activated kinase inhibitor PF-3758309 is a potent inhibitor of oncogenic signaling and tumor growth. *Proc. Natl. Acad. Sci. U.S.A.* **107,** 9446–9451
33. Deacon, S. W., Beeser, A., Fukui, J. A., Rennefahrt, U. E. E., Myers, C., Chernoff, J., and Peterson, J. R. (2008) An isoform-selective, small-molecule inhibitor targets the autoregulatory mechanism of p21-activated kinase. *Chem. Biol.* **15,** 322–331
34. Callow, M. G., Zozulya, S., Gishizky, M. L., Jallal, B., and Smeal, T. (2005) PAK4 mediates morphological changes through the regulation of GEF-H1. *J. Cell Sci.* **118,** 1861–1872
35. Curmi, P. A., Andersen, S. S. L., Lachkar, S., Gavet, O., Karsenti, E., Knossow, M., and Sobel, A. (1997) The stathmin/tubulin interaction *in vitro*. *J. Biol. Chem.* **272,** 25029–25036
36. Gavet, O., Ozon, S., Manceau, V., Lawler, S., Curmi, P., and Sobel, A. (1998) The stathmin phosphoprotein family: intracellular localization and effects on the microtubule network. *J. Cell Sci.* **111,** 3333–3346
37. Küntziger, T., Gavet, O., Manceau, V., Sobel, A., and Bornens, M. (2001) Stathmin/Op18 phosphorylation is regulated by microtubule assembly. *Mol. Biol. Cell* **12,** 437–448
38. Wittmann, T., Bokoch, G. M., and Waterman-Storer, C. M. (2004) Regulation of microtubule destabilizing activity of Op18/stathmin downstream of Rac1. *J. Biol. Chem.* **279,** 6196–6203
39. Roig, J., and Traugh, J. A. (1999) p21-activated protein kinase γ-PAK is activated by ionizing radiation and other DNA-damaging agents. *J. Biol. Chem.* **274,** 31119–31122
40. Huang, Z., Ling, J., and Traugh, J. A. (2003) Localization of p21-activated protein kinase-γ-PAK/Pak2 in the endoplasmic reticulum is required for induction of cytostasis. *J. Biol. Chem.* **278,** 13101–13109
41. Dharmawardhane, S., Brownson, D., Lennartz, M., and Bokoch, G. M. (1999) Localization of p21-activated kinase 1 (PAK1) to pseudopodia, membrane ruffles, and phagocytic cups in activated human neutrophils. *J. Leukocyte Biol.* **66,** 521–527
42. Tao, J., Oladimeji, P., Rider, L., and Diakonova, M. (2011) PAK1-Nck regulates cyclin D1 promoter activity in response to prolactin. *Mol. Endocrinol.* **25,** 1565–1578

Downloaded from www.jbc.org at Istituto Superiore di Sanità, on April 1, 2013